Analysis and Design of a 45° Slant-Polarized Omnidirectional Antenna

XuLin Quan, RongLin Li, *Senior Member, IEEE*, Yi Fan, and Dimitris E. Anagnostou, *Senior Member, IEEE*

***Abstract*—A 45° slant-polarized omnidirectional antenna is proposed for mobile communication base stations. The proposed antenna consists of four printed crossed-dipole elements which are rolled up into a cylinder for omnidirectional radiation. Each crossed-dipole element is composed of a horizontal dipole and a vertical dipole. The 45° slant polarization is achieved by adjusting the lengths of the horizontal and vertical dipoles. A broadband feeding network consisting of four broadband baluns and an impedance matching circuit is introduced to feed the four crossed-dipole elements. Experimental results show that the omnidirectionality or gain variation in the horizontal plane is less than 1 dB while the cross-polarization level is below −15 dB over a bandwidth of 15% (1.9–2.2 GHz). The 45° slant-polarized omnidirectional antenna has a bandwidth of 22% (1.75–2.18 GHz) for 15-dB return loss. Theoretical analysis and design procedure are presented.**

***Index Terms*—45° slant polarization, base station antenna, mobile communications, omnidirectional antenna.**

I. Introduction

In a mobile communication system, base station antennas with $\pm 45^\circ$ slant polarization are commonly used because this type of polarization scheme offers more symmetrical propagation characteristics than vertical/horizontal polarization does [1]. A number of antennas have been proposed for 45° slant-polarized antenna [2]–[5]. However, all of these 45° slant-polarized antennas have a unidirectional radiation pattern which covers a sector (e.g., 120°) of azimuthal plane in a cellular system. For 360° coverage, antennas with an omnidirectional radiation pattern are required. It is well known that a vertically polarized omnidirectional antenna can be realized by a vertical dipole [6], while a horizontally polarized omnidirectional antenna may be obtained by a horizontal loop [7], [8]. A vertical/horizontal dual-polarized omnidirectional slot antenna was proposed in [9], but it is not 45° slant-polarized. For a 45° slant-polarized omnidirectional antenna, it is necessary to have an omnidirectional radiation pattern with equal horizontal and vertical components, including the same magnitude and the same phase. To the best of our knowledge, there are very few publications reporting 45° slant-polarized omnidirectional antennas. In [10], a bifilar helix antenna was claimed to be a 45° slant-polarized omnidirectional antenna. Unfortunately, it has been verified that this antenna is actually a circularly polarized omnidirectional antenna [11].

In this paper, a real 45° slant-polarized omnidirectional antenna is proposed. This antenna consists of four crossed-dipole elements which are wrapped around a cylinder for an omnidirectional radiation pattern. Each crossed-dipole element includes a horizontal dipole and a vertical dipole. The 45° slant polarization is realized by adjusting the lengths of the horizontal and vertical dipoles. A feeding network composed of four broadband baluns and an impedance matching circuit is designed to excite the 45° slant-polarized omnidirectional antenna, achieving a bandwidth of 22% (1.75–2.18 GHz) for 15-dB return loss. The cross-polarization level is below -15 dB and gain variation (or omnidirectionality [12]) is less than 1 dB (peak-to-peak) in the horizontal plane over a bandwidth of 15% (1.9–2.2 GHz).

Section II describes the configuration of the 45° slant-polarized omnidirectional antenna. Analysis and design are presented in Section III. An experimental verification is demonstrated in Section IV.

II. Antenna Configuration

The configuration of a 45° slant-polarized omnidirectional antenna is depicted in Fig. 1. The antenna includes four crossed-dipole elements and a feeding network. The four crossed-dipole elements are first printed on a thin flexible dielectric substrate and then rolled up into a hollow cylinder of diameter D (see Fig. 1(a)) to achieve an omnidirectional radiation pattern. Each crossed-dipole element is composed of a horizontal dipole and a vertical dipole (see Fig. 1(b)), which have lengths L_h and L_v, respectively. The 45° slant polarization is achieved by adjusting the lengths L_h and L_v. (Note that four 45° slanted dipoles cannot radiate an omnidirectional pattern with 45° slant polarization; instead they may generate a circularly polarized omnidirectional pattern [13], [14].) Four crossed-dipole elements are excited through a feeding network that comprises four broadband baluns and an impedance matching circuit (see Fig. 1(c)). A 50-Ω coaxial line is connected to the feeding network at the "Feeding point".

The 45° slant-polarized omnidirectional antenna was designed for UMTS (1.92–2.17 GHz) base stations at a center frequency of 2.05 GHz. The design procedure will be described

Manuscript received December 30, 2012; revised October 08, 2013; accepted October 23, 2013. Date of publication November 01, 2013; date of current version December 31, 2013. This work was supported in part by the National Natural Science Foundation of China (61372009), in part by the Fundamental Research Funds for the Central Universities (2013ZP0022), in part by the Defense Advanced Research Projects Agency/Microsystems Technology Office (MTO) Young FacultyAward No. N66001-11-1-4145, in part by the Air Force Research Laboratories/SAIC under Contract No. FA9453-08-C-0245, and in part by the National Science Foundation underGrant No. ECS-1310400.

X.L. Quan, R.L. Li, and Y. Fan are with the School of Electronic and Information Engineering, South China University of Technology, Guangzhou 510641, China (e-mail: lirl@scut.edu.cn).

D. E. Anagnostou is with the South Dakota School of Mines and Technology, Rapid City, SD 57701 USA and also with the Democritus University of Thrace, Xanthi 67100, Greece.

Color versions of one or more of the figures in this paper are available online at http://ieeexplore.ieee.org.

Digital Object Identifier 10.1109/TAP.2013.2288367

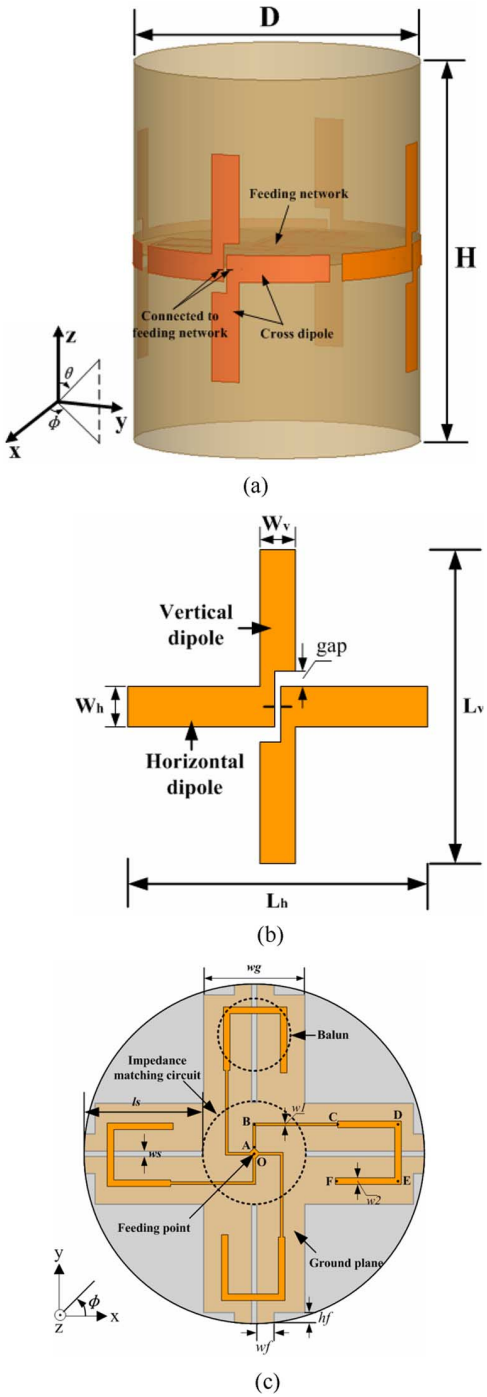

Fig. 1. Configuration of a 45° slant-polarized omnidirectional antenna: (a) Perspective view; (b) Crossed-dipole element; (c) Feeding network.

in the next section. The 45° slant-polarized omnidirectional antenna was simulated using Ansoft HFSS v13. The geometric parameters of the simulated antenna are listed in Table I.

III. Analysis and Design

To understand the operating mechanism of the 45° slant-polarized omnidirectional antenna, we first define ±45° slant-polarized electric field components as follows [15]:

$$E_{+45^\circ} = E_\phi \cos 45^\circ - E_\theta \sin 45^\circ \quad (1)$$

$$E_{-45^\circ} = E_\phi \cos 45^\circ + E_\theta \sin 45^\circ \quad (2)$$

TABLE I
Geometric Parameters for the 45° Slant-Polarized Antenna

Parameter	Value (mm)	Parameter	Value (mm)
D	77.6	CD	13.7
H	100.0	DE	13.0
L_h	59.0	EF	14.3
W_h	8.0	w_1	0.6
L_v	64.0	w_2	1.5
W_v	7.0	ls	27.0
gap	3.0	ws	1.2
w_g	23.0	h_f	2.5
OB	6.7	w_f	4.5
BC	19.0		

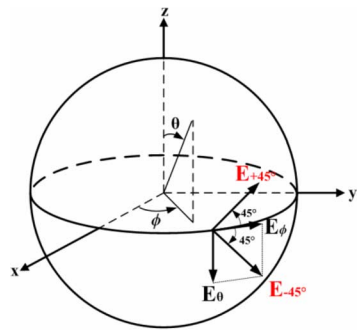

Fig. 2. Definition of 45° slant-polarized components.

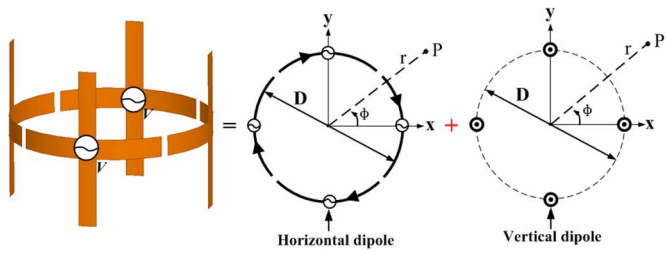

Fig. 3. Four crossed-dipole elements decomposed into four horizontal arc dipoles plus four vertical dipoles.

where E_θ and E_ϕ are the θ and ϕ components of the far-zone electric field, respectively, as illustrated in Fig. 2. Obviously, it is required for a purely 45° slant polarization to meet two conditions: 1) the magnitudes of E_θ and E_ϕ need to be equal, i.e., $|E_\theta| = |E_\phi|$; 2) the phases of E_θ and E_ϕ can be equal, i.e., $\angle E_\theta = \angle E_\phi$, or have a 180° phase difference, i.e., $\angle E_\theta - \angle E_\phi = 180^\circ$. For +45° slant polarization, $|E_\theta| = |E_\phi|$ and $\angle E_\theta - \angle E_\phi = 180^\circ$, while for −45° slant polarization, $|E_\theta| = |E_\phi|$ and $\angle E_\theta = \angle E_\phi$.

Four rolled crossed-dipole elements can be decomposed into four horizontal arc dipoles plus four vertical straight dipoles, as shown in Fig. 3. To simplify the analytical procedure, we replace the four horizontal arc dipoles with four straight dipoles, as illustrated in Fig. 4.

It is assumed that the current distribution on every dipole is sinusoidal. The far-zone electric field radiated by four vertical dipoles in the horizontal plane (i.e., $\theta = 90^\circ$) is (see Appendix)

$$E_\theta = j\frac{120 I_v e^{-jkr}}{r}\left(1-\cos\left(\frac{kL_v}{2}\right)\right)\left[\cos\left(\frac{kD}{2}\cos\phi\right) + \cos\left(\frac{kD}{2}\sin\phi\right)\right] \quad (3)$$

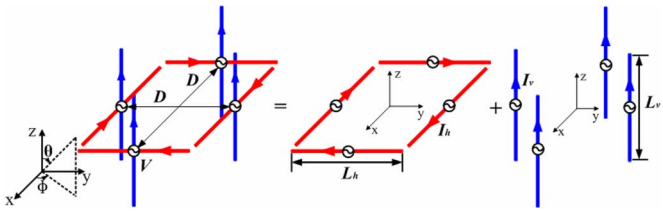

Fig. 4. Simplified crossed-dipole elements and associated decomposition.

where I_v is the amplitude of the sinusoidal current on the vertical dipoles and $k = 2\pi/\lambda$ is the wave number with $\lambda =$ wavelength in free space at the center frequency of an operating frequency band.

Similarly, the electric field radiated by four horizontal dipoles in the horizontal plane (i.e., $\theta = 90°$) can be found to be (also see Appendix)

$$E_\phi = -\frac{120 I_h e^{-jkr}}{r}\left\{\frac{\sin\left(\frac{kD}{2}\sin\phi\right)}{\sin\phi} \times \left(\cos\left(\frac{kL_h}{2}\cos\phi\right) - \cos\left(\frac{kL_h}{2}\right)\right) + \frac{\sin\left(\frac{kD}{2}\cos\phi\right)}{\cos\phi}\left(\cos\left(\frac{kL_h}{2}\sin\phi\right) - \cos\left(\frac{kL_h}{2}\right)\right)\right\} \quad (4)$$

where I_h is the amplitude of the sinusoidal current on the horizontal dipoles.

There are three critical parameters for the 45° slant-polarized omnidirectional antenna, including the diameter of the hollow cylinder (D) and the lengths of the horizontal and vertical dipoles (L_h and L_v), which are determined as follows.

A. Determination of Antenna Diameter (D)

According to the definition of 45° slant polarization, the first necessary condition is $|E_\theta| = |E_\phi|$, or $|E_\theta|/|E_\phi| = 1$. We calculate $|E_\theta|/|E_\phi|$ using (3) and (4) for a dipole length of a half-wavelength (i.e., $L_v = L_h = \lambda/2$) and plot $|E_\theta|/|E_\phi|$ as a function of the azimuthal angle ϕ for difference values of the antenna diameter (D) in Fig. 5. It can be seen that when $D = 0.6\lambda$, $|E_\theta|/|E_\phi|$ varies around 0.6 and the variation (peak-to-peak) is larger than 0.3. When $D = 0.4\lambda$, the variation is less than 0.1 but $|E_\theta|/|E_\phi|$ is larger than 1.3. As D is close to a half-wave length, $|E_\theta|/|E_\phi|$ is close to 1. The optimal value for the antenna diameter is $D = 0.475\lambda$ at which $|E_\theta|/|E_\phi|$ varies around 1 and the variation is less than 0.2. Note that this optimal value is found for the simplified crossed-dipole elements with straight horizontal dipole.

For the original crossed-dipole elements with horizontal arc dipoles, the antenna diameter should be slightly larger than 0.475λ. By simulation, the optimized antenna diameter is found to be close to a half-wave length, i.e., $D \cong 0.5\lambda$.

B. Determination of Lengths (L_h and L_v)

Based on the definition of 45° slant polarization, the second necessary condition requires the phases of E_θ and E_ϕ to be equal, i.e., $\angle E_\theta = \angle E_\phi$, or to have a 180° difference, i.e., $\angle E_\theta - \angle E_\phi = 180°$. From (3) and (4), we can see that E_θ and E_ϕ would have a 90° phase difference if the current (I_h) on the horizontal dipoles is in phase with the current (I_v) on the vertical dipoles. The currents (I_h and I_v) depend on the phase $(\angle Z_{in})$ of the input impedance Z_{in} of each dipole, which varies with the length of the dipole. Fig. 6 shows the phase $\angle Z_{in}$ simulated for a printed dipole with width $w = 0.05\lambda$ as a function of the dipole length l. It is seen that a 90° phase difference can be obtained by changing the length l approximately from $l = 0.35\lambda$ to $l = 0.5\lambda$. This means that the lengths of the horizontal and vertical dipoles (L_h and L_v) can be chosen to be $L_h = \sim 0.35\lambda$ and $L_v = \sim 0.5\lambda$.

Considering the mutual coupling and the actual current distributions on the crossed-dipole elements, we optimized the lengths L_h and L_v by simulation. Fig. 7 shows the magnitude ratio $(|E_\theta|/|E_\phi|)$ and phase difference $(\angle E_\theta - \angle E_\phi)$ as a function of L_v for different values of L_h. From Figs. 7(a) and (c), it is seen that when $L_h = 0.375\lambda$ and 0.425λ, it is impossible to satisfy the conditions $|E_\theta|/|E_\phi| = 1$ and $\angle E_\theta - \angle E_\phi = 180°$ for the same L_v. This implies that 45° slant polarization cannot be achieved for $L_h = 0.375\lambda$ and 0.425λ. From Fig. 7(b), it can be seen that when $L_h = 0.4\lambda$ and $L_v = 0.45\lambda$, both the

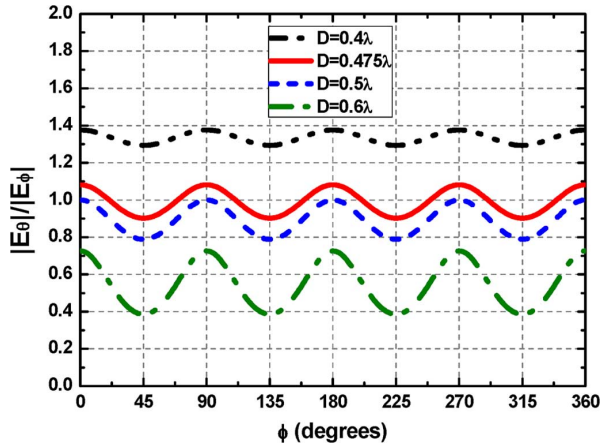

Fig. 5. $|E_\theta|/|E_\phi|$ for different values of the antenna diameter (D).

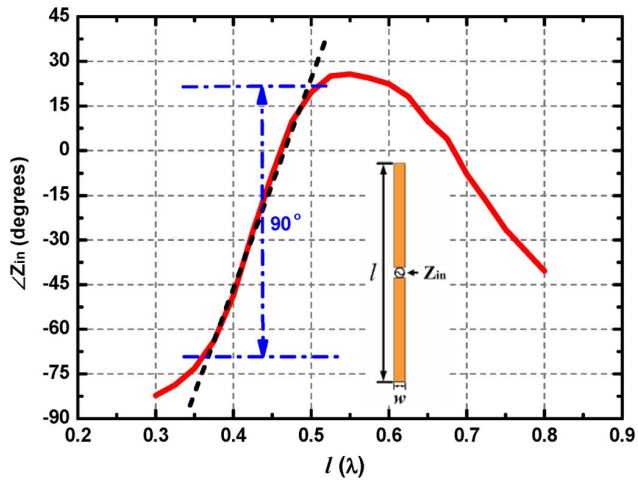

Fig. 6. The phase $\angle Z_{in}$ of the input impedance Z_{in} for a printed dipole as a function of the dipole length l.

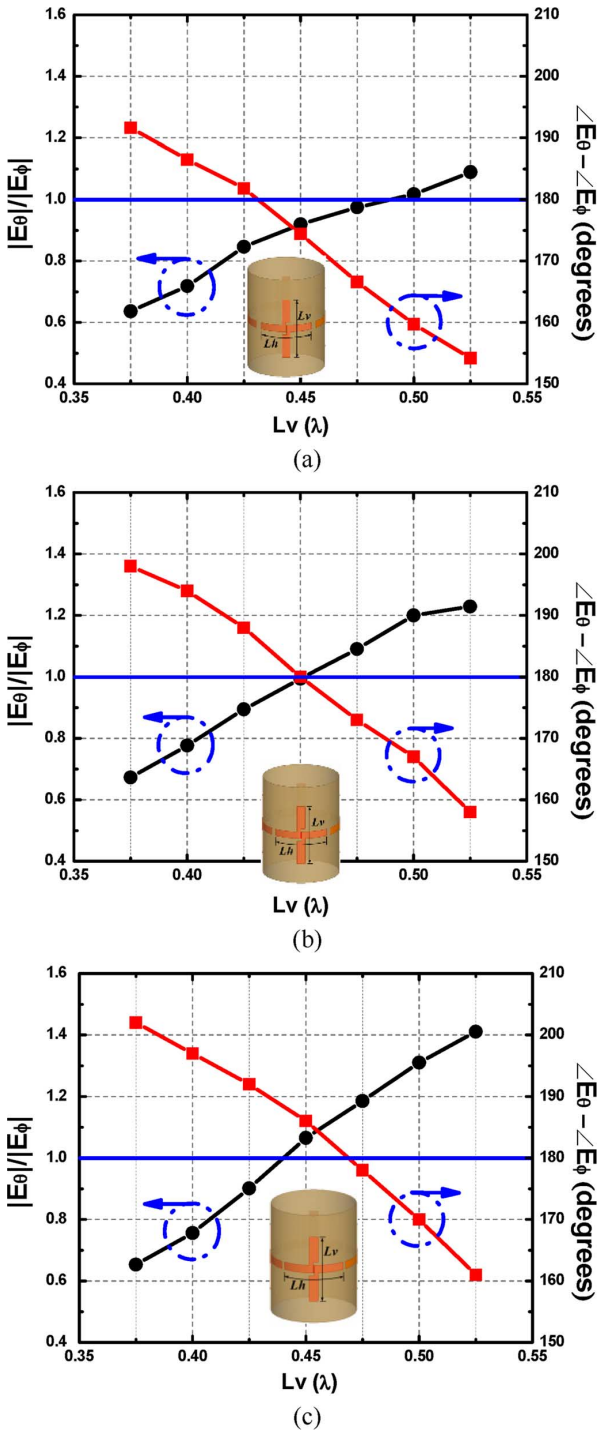

Fig. 7. Magnitude ratio ($|E_\theta|/|E_\phi|$) and phase difference ($\angle E_\theta - \angle E_\phi$) as a function of L_v for different values of L_h: (a) $L_h = 0.375\lambda$; (b) $L_h = 0.4\lambda$; (c) $L_h = 0.425\lambda$.

conditions $|E_\theta|/|E_\phi| = 1$ and $\angle E_\theta - \angle E_\phi = 180°$ are satisfied; thus $+45°$ slant polarization can be achieved. For $-45°$ slant polarization, it is easy to be obtained by switching the connecting points between the horizontal and vertical dipoles. Fig. 8 demonstrates the magnitude ratio ($|E_\theta|/|E_\phi|$) and phase difference ($\angle E_\theta - \angle E_\phi$) as a function of frequency for the optimized lengths $L_h = 0.4\lambda$ and $L_v = 0.45\lambda$. It is seen that $|E_\theta|/|E_\phi| = 1 \pm 0.2$ and $\angle E_\theta - \angle E_\phi = 180 \pm 4°$ over the frequency range 1.9–2.2 GHz.

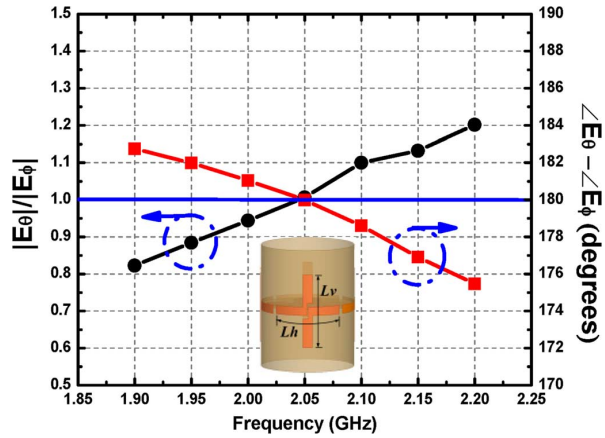

Fig. 8. Magnitude ratio ($|E_\theta|/|E_\phi|$) and phase difference ($\angle E_\theta - \angle E_\phi$) as a function of frequency for $L_h = 0.4\lambda$ and $L_v = 0.45\lambda$.

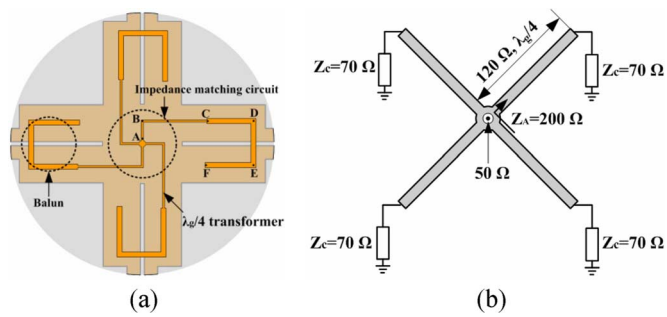

Fig. 9. Feeding network (a) and its equivalent circuit (b) for the 45° slant-polarized omnidirectional antenna.

C. Feeding Network

A feeding network consisting of four broadband baluns and an impedance matching circuit is introduced to feed the four crossed-dipole elements. The input impedance of the broadband balun for each crossed-dipole element (e.g., looking at Point "C" in Fig. 9(a)) is designed to be 70 Ω. The theoretical analysis of the broadband balun can be found in [16]. To match four broadband baluns connected in parallel to a 50-Ω coaxial line, an impedance matching circuit is needed. An equivalent circuit for the impedance matching is depicted in Fig. 9(b). The broadband balun was simplified as a 70-Ω impedance The 70-Ω impedance looking at Point "C" ($Z_C = 70\ \Omega$) is transformed into a 200-Ω impedance at Point "A" ($Z_A = 200\ \Omega$) by a 120-Ω quarter-wave ($\lambda_g/4$) transformer ($\sqrt{200\ \Omega \times 70\ \Omega} = 120\ \Omega$). Then the four 200-Ω impedances are connected in parallel, resulting in a 50-Ω impedance, matching to the 50-Ω coaxial line at the center of the feeding network. The simulated input impedances from 1.7–2.2 GHz at different points of the feeding network are shown in Fig. 10. It can be seen that the input impedance for each crossed-dipole element (Z_{dipole}) is capacitive. After impedance transformation through the slot-line coupling, the impedance (Z_c) at Point "C" is approximately equal to 70 Ω at the center frequency 2.05 GHz. Following the quarter-wave transformer, the total input impedance (Z_{in}) of the feeding network is matched to 50 Ω.

IV. Experimental Verification

To verify the design, the 45° slant-polarized omnidirectional antenna was fabricated and measured. Fig. 11 shows a picture

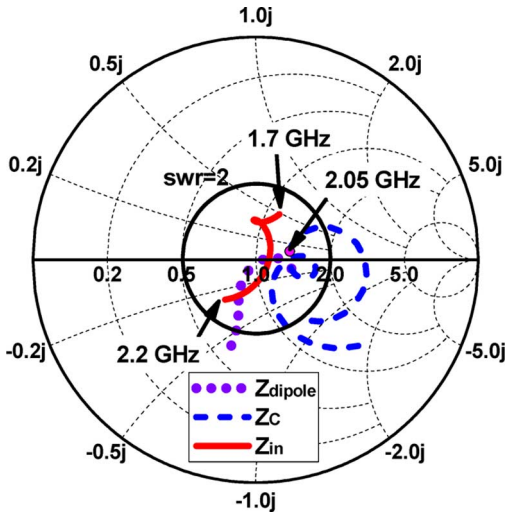

Fig. 10. Simulated input impedances at different points of the feeding network.

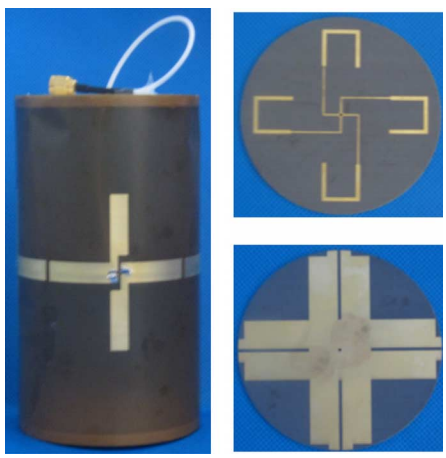

Fig. 11. A picture of the prototype of a 45° slant-polarized omnidirectional antenna with feeding network.

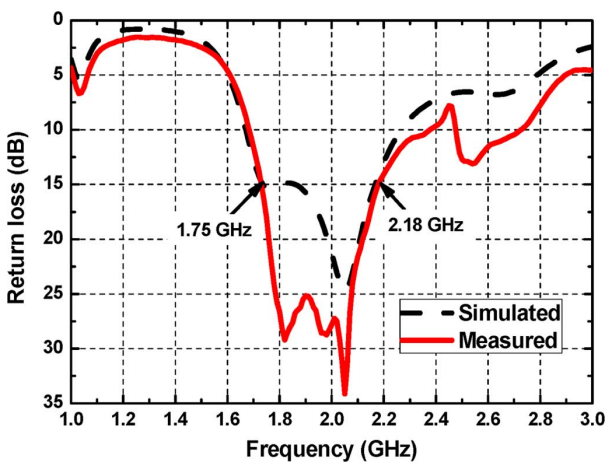

Fig. 12. Simulated and measured results for return loss of the 45° slant-polarized omnidirectional antenna.

of the antenna prototype with the front and back views of the feeding network. Four crossed-dipole elements were first printed on a Panasonic R-F775 flexible dielectric substrate ($\varepsilon_r = 3.2$, loss tangent $= 0.0015$, thickness $= 0.05$ mm)

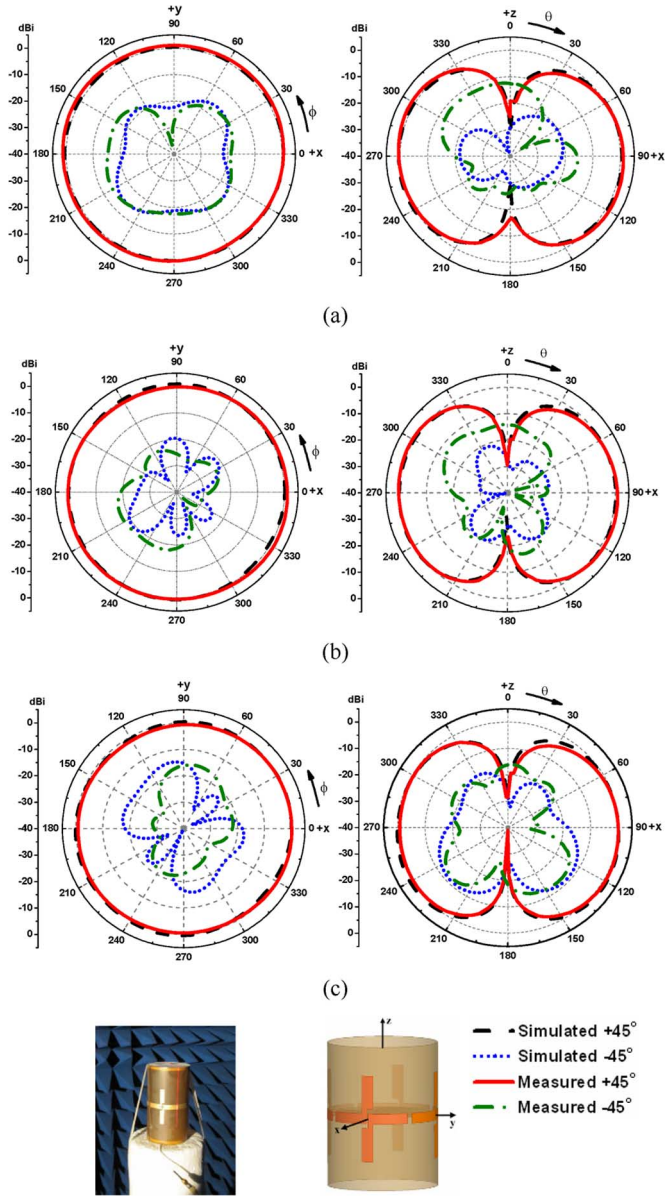

Fig. 13. Simulated and measured radiation patterns of the 45° slant-polarized omnidirectional antenna at (a) 1.9 GHz, (b) 2.05 GHz, and (c) 2.2 GHz.

and then rolled up into a hollow cylinder. The feeding network was printed on a Taconic TLY-5 dielectric substrate ($\varepsilon_r = 2.2$, loss tangent $= 0.0009$, thickness $= 0.8$ mm). A flexible coaxial line (Johnson/Emerson RG178) with an SMA connector is connected to the feeding network.

Fig. 12 shows simulated and measured results of return loss (RL). Good agreement is observed. The measured bandwidth for RL > 15 dB is about 22% (1.75 GHz–2.18 GHz). The radiation patterns of the 45° slant-polarized omnidirectional antenna simulated and measured at 1.9, 2.05, and 2.2 GHz are plotted in Fig. 13. The radiation pattern was measured using a SATIMO antenna measurement system SG24 at the Speed Communication Technology Corporation Ltd., Shenzhen, China. It is observed that the gain variation in the horizontal plane (i.e., the x-y plane) is less than 1 dB, confirming a good omnidirectionality. The cross-polarization level (i.e., the $-45°$ polarized component) is -15 dB below the co-polarization (i.e., the $+45°$ po-

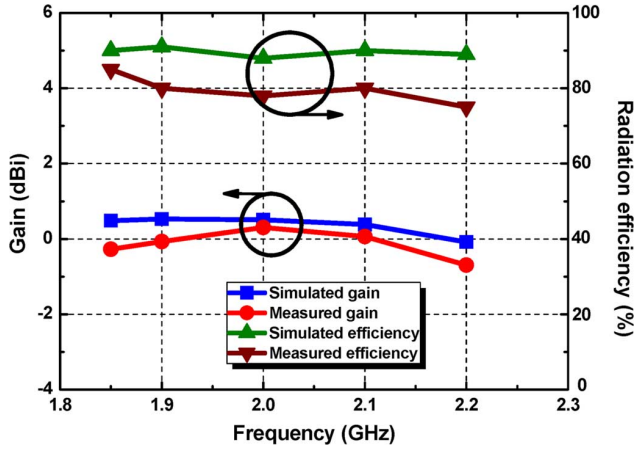

Fig. 14. Gain and radiation efficiency for the 45° slant-polarized omnidirectional antenna.

larized component) in the horizontal plane. Fig. 14 presents the simulated and measured gains of the 45° slant-polarized omnidirectional antenna. The measured gain is around 0 dBi, which is lower than the gain of a typical half-wave dipole antenna. The lower gain is mainly due to the broader beamwidth in the elevation plane, which is found to be ~120° (half-power beamwidth), much wider than 78° for a half-wave dipole. The radiation efficiency of the 45° slant-polarized omnidirectional antenna is about 80% (also see Fig. 14). The simulated efficiency is slightly higher than measured result because the simulation did not take the feeding coaxial line into account.

V. Conclusion

A 45° slant-polarized omnidirectional antenna is developed by utilizing four crossed-dipole elements. The operating mechanism and design method are elaborated. The 45° slant-polarized omnidirectional antenna achieves a bandwidth of 22% (1.75–2.18 GHz) for 15-dB return loss. The gain variation is less than 1 dB and the cross-polarization level is below −15 dB over a bandwidth of 15% (1.9–2.2 GHz). This broadband omnidirectional antenna may find applications in base stations for mobile communications.

Appendix
Derivation of E_θ in (3) and E_ϕ in (4)

Consider a vertical dipole of length L placed coincidently with the z axis and with its center at the origin. Assume a sinusoidal current distribution on the dipole. The far-zone electric field for the vertical dipole in the horizontal plane (i.e., $\theta = 90°$) is given by [6], [17]

$$E_\theta = j\eta \frac{I_0}{2\pi r}\left(1-\cos\left(\frac{kL}{2}\right)\right)e^{-jkr} \tag{A1}$$

where I_0 is the amplitude of the sinusoidal current on the dipoles and $\eta \cong 120\pi$ is the intrinsic impedance of the free space.

For four vertical dipoles equally spaced along a circular ring of radius R, as shown in Fig. A1, the far-zone electric field in the horizontal plane for each dipole can be approximately expressed for r ≫ R as

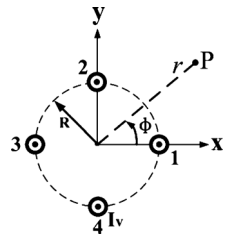

Fig. A1. Four vertical dipoles.

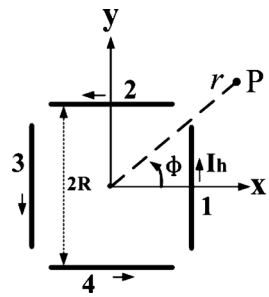

Fig. A2. Four horizontal dipoles.

$$E_{\theta 1} = j\eta \frac{I_v e^{-jkr}}{2\pi r}\left(1-\cos\left(\frac{kL}{2}\right)\right)e^{jkR\cos\phi} \tag{A2}$$

$$E_{\theta 2} = j\eta \frac{I_v e^{-jkr}}{2\pi r}\left(1-\cos\left(\frac{kL}{2}\right)\right)e^{jkR\sin\phi} \tag{A3}$$

$$E_{\theta 3} = j\eta \frac{I_v e^{-jkr}}{2\pi r}\left(1-\cos\left(\frac{kL}{2}\right)\right)e^{-jkR\cos\phi} \tag{A4}$$

$$E_{\theta 4} = j\eta \frac{I_v e^{-jkr}}{2\pi r}\left(1-\cos\left(\frac{kL}{2}\right)\right)e^{-jkR\sin\phi} \tag{A5}$$

Thus, the total electric field is the sum of fields from the four vertical dipoles as given by (3).

For four horizontal dipoles placed along a square of side length 2R, as shown in Fig. A2, the far-zone electric field in the horizontal plane for each dipole can be found to be

$$E_{\phi 1} = -j\eta \frac{I_h e^{-jkr}}{2\pi r}\frac{1}{\cos\phi}\left(\cos\left(\frac{kL}{2}\sin\phi\right) - \cos\left(\frac{kL}{2}\right)\right)e^{jkR\cos\phi} \tag{A6}$$

$$E_{\phi 2} = -j\eta \frac{I_h e^{-jkr}}{2\pi r}\frac{1}{\sin\phi}\left(\cos\left(\frac{kL}{2}\cos\phi\right) - \cos\left(\frac{kL}{2}\right)\right)e^{jkR\sin\phi} \tag{A7}$$

$$E_{\phi 3} = j\eta \frac{I_h e^{-jkr}}{2\pi r}\frac{1}{\cos\phi}\left(\cos\left(\frac{kL}{2}\sin\phi\right) - \cos\left(\frac{kL}{2}\right)\right)e^{-jkR\cos\phi} \tag{A8}$$

$$E_{\phi 4} = j\eta \frac{I_h e^{-jkr}}{2\pi r}\frac{1}{\sin\phi}\left(\cos\left(\frac{kL}{2}\cos\phi\right) - \cos\left(\frac{kL}{2}\right)\right)e^{-jkR\sin\phi} \tag{A9}$$

Therefore, the sum of electric fields from the four horizontal dipoles leads to the total electric field given by (4).

ACKNOWLEDGMENT

The authors would like to thank Speed Communication Technology Corporation Ltd., Shenzhen, China, for radiation pattern measurement. They would also like to thank three anonymous reviewers for their valuable comments which made the paper more readable.

REFERENCES

[1] B. Lindmark and M. Nilsson, "On the available diversity gain from different dual-polarized antennas," *IEEE J. Sel. Areas Commun.*, vol. 19, no. 2, pp. 287–294, 2001.

[2] M. Hajj, R. Chantalat, T. Monédière, and B. Jecko, "A 45° linearly polarized sectoral antenna with M-EBG structure for WiMAX base stations," *IEEE Antennas Propag. Lett.*, vol. 9, pp. 737–740, 2010.

[3] K. Gosalia and G. Lazzi, "Reduced size dual polarized microstrip patch antenna for wireless communications," *IEEE Trans. Antennas Propag.*, vol. 51, no. 9, pp. 2182–2186, 2003.

[4] Q. F. Zhang and Y. L. Lu, "45° linearly polarized substrate integrated waveguide-fed slot array antennas," in *Proc. Int. Conf. Microwave and Millimeter Wave Technology (ICMMT)*, 2008, pp. 1214–1217.

[5] V. F. Fusco and P. H. Rao, "Wide-band slant linearly polarized antenna," *IEEE Trans. Antennas Propag.*, vol. 51, no. 8, pp. 2014–2019, 2003.

[6] C. A. Balanis, *Antenna Theory Analysis and Design*, 3rd ed. Hoboken, NJ, USA: Wiley-Interscience, 2005, pp. 170–184.

[7] X. Quan, R. Li, J. Wang, and Y. Cui, "Development of a broadband horizontally polarized omnidirectional planar antenna and its array for base stations," *Progr. Electromagn. Res.*, vol. 128, pp. 441–456, 2012.

[8] K. Wei, Z. Zhang, Z. Feng, and M. F. Iskander, "A MNG-TL loop antenna array with horizontally polarized omnidirectional patterns," *IEEE Trans. Antennas Propag.*, vol. 60, no. 6, pp. 2702–2710, 2012.

[9] Y. Li, Z. J. Zhang, J. F. Zheng, and Z. H. Zheng, "Compact azimuthal omnidirectional dual-polarized antenna using highly isolated colocated slots," *IEEE Trans. Antennas Propag.*, vol. 60, no. 9, pp. 4037–4045, 2012.

[10] M. Amin, R. Cahill, and V. Fusco, "Single feed low profile omnidirectional antenna with slant 45 linear polarization," *IEEE Trans. Antennas Propag.*, vol. 55, no. 11, pp. 3087–3090, 2007.

[11] S. Iqbal, M. Amin, and J. Yousaf, "Low profile circularly polarized side-fed bifilar helix antenna," in *Proc. Int. Bhurban Conf. on Applied Sciences and Technology*, 2012, pp. 325–328.

[12] N. Herscovici, Z. Sipus, and P.-S. Kildal, "The cylindrical omnidirectional patch antenna," *IEEE Trans. Antennas Propag.*, vol. 49, no. 12, pp. 1746–1753, Dec. 2001.

[13] G. H. Brown and O. M. Woodward, "Circularly polarized omnidirectional antenna," *RCA Rev.*, vol. 8, pp. 259–269, 1947.

[14] Y. M. Pan and K. W. Leung, "Wideband omnidirectional circularly polarized dielectric resonator antenna with parasitic strips," *IEEE Trans. Antennas Propag.*, vol. 60, no. 6, pp. 2992–2997, Jun. 2012.

[15] M. Tian, "Radiation characterization of slant polarization antennas," *Microwave Journal*, May 1999.

[16] R. L. Li, T. Wu, B. Pan, K. Lim, J. Laskar, and M. M. Tentzeris, "Equivalent-circuit analysis of a broadband printed dipole with adjusted integrated balun and array for base station applications," *IEEE Trans. Antennas Propag.*, vol. 57, pp. 2180–2184, Jul. 2009.

[17] J. D. Kraus and R. J. Marhefka, *Antennas: For All Applications*, 3rd ed. New York, NY, USA: McGraw Hill Science, 2002, pp. 177–181.

XuLin Quan was born in Henan, China, in 1987. She received the B.S. degree from the School of Information Engineering, Zhengzhou University, Zhengzhou, China, in 2004. She is currently working toward the Ph.D. degree at South China University of Technology.

Her current research interests include microwave engineering and technologies for wireless communications.

RongLin Li (M'02–SM'03) received the B.S. degree in electrical engineering from Xi'an Jiaotong University, China, in 1983, and the M.S. and Ph.D. degrees in electrical engineering from Chongqing University, in 1990 and 1994, respectively.

From 1983 to 1987, he worked as an Assistant Electrical Engineer at the Yunnan Electric Power Research Institute. From 1994 to 1996, he was a Postdoctoral Research Fellow in Zhejiang University, China. In 1997, he visited Hosei University, Japan, as an HIF (Hosei International Fund) Research Fellow. In 1998, he became a Professor at Zhejiang University. In 1999, he visited the University of Utah, USA, as a Research Associate. In 2000, he worked as a Research Fellow at the Queen's University of Belfast, UK. Since 2001, he has been a Research Scientist at the Georgia Institute of Technology, USA. He is now an Endowed Professor in the South China University of Technology. He has published more than 100 papers in refereed Journals and Conference Proceedings, and three book chapters. His current research interests include new design techniques for antennas in mobile and satellite communication systems, phased arrays and smart antennas for radar applications, wireless sensors and RFID technology, electromagnetics and information theory.

Dr. Li is a member of the IEEE International Compumag Society. He was the recipient of the 2009 Georgia Tech-ECE Research Spotlight Award. He currently serves as an Editor of the *ETRI Journal* and a reviewer for a number of international journals, including the IEEE TRANSACTIONS ON ANTENNAS AND PROPAGATION, *IEEE Antennas and Wireless Propagation Letters, IEEE Microwave and Wireless Components Letters, IET Microwave, Antennas & Propagation, Progress in Electromagnetic Research, Journal of Electromagnetic Waves and Applications*, and *International Journal of Wireless Personal Communications*. He was a member of the Technical Program Committee for IEEE-IMS 2008–2012 Symposia and a Session Chair for several IEEE-APS Symposia.

Yi Fan was born in Guangxi, China, in 1976. She received the B.S. degree in electrical engineering from Chongqing University, China, in 1998, and the M.S. degree in circuits and systems from South China University of Technology, Guangzhou, China, in 2005, where she is currently working toward the Ph.D. degree.

Her current research interests include omnidirectional antennas and reconfigurable antennas.

Dimitris E. Anagnostou (S'98–M'05–SM'10) received the B.S.E.E. degree from the Democritus University of Thrace, Greece, in 2000, and the M.S.E.E. and Ph.D. degrees from the University of New Mexico, Albuquerque, NM, USA, in 2002 and 2005, respectively.

From 2005 to 2006, he was a Postdoctoral Fellow at the Georgia Institute of Technology, Atlanta, GA, USA. In 2007, he joined the faculty of the Electrical and Computer Engineering Department, South Dakota School of Mines and Technology, Rapid City, SD, USA, as an Assistant Professor and became an Associate Professor in 2013. He has authored or coauthored 81 papers published in refereed journals and symposia proceedings and he holds one U.S. patent on reconfigurable antennas. His interests include reconfigurable, autonomous, flexible, electrically-small and miniaturized antennas and arrays; phase-change materials; analytical design methods and equivalent circuits of antennas and microwave components; metamaterial applications; direct-write; "green" RF electronics on paper and organic substrates; applications of artificial dielectrics and superstrates; antennas on PV-cells; RF-MEMS; propagation in tunnels; and microwave packaging.

Dr. Anagnostou is a member of Eta Kappa Nu, ASEE, and of the Technical Chamber of Greece. He was the recipient of the 2011 DARPA Young Faculty Award and the 2010 IEEE Antennas and Propagation Society (AP-S) John Kraus Antenna Award. He also received the 2011 AFRL Summer Faculty Fellowship by the ASEE, the Honored Faculty Achievement by SDSMT in 2010, 2011, 2012 and 2013. In 2006, he was recognized as a Distinguished Scientist Living Abroad by the Hellenic Ministry of Defense. He serves as Associate Editor for the IEEE TRANSACTIONS ON ANTENNAS AND PROPAGATION and the *Springer International Journal of Machine Learning and Cybernetics*. He is a member of the IEEE APS Educational Committee, the TPC and Session Chair for IEEE APS International Symposia, and is a reviewer for 15 international journal publications including the IEEE T-AP, T-MTT, AP-S Magazine, AWPL, and MWCL. He has given two workshop presentations at IEEE AP-S and IEEE MTT-S International Symposia.